journal

J. Am. Ceram. Soc., 85 [10] 2417–24 (2002)

Self-Propagating High-Temperature Synthesis of Ti_3SiC_2: I, Ultra-High-Speed Neutron Diffraction Study of the Reaction Mechanism

Daniel P. Riley and Erich H. Kisi

Department of Mechanical Engineering, The University of Newcastle, Callaghan, NSW 2308, Australia

Thomas C. Hansen and Alan W. Hewat

Institut Max von Laue-Paul Langevin, 38042 Grenoble, Cedex 9, France

In situ **neutron diffraction at 0.9 s time resolution was used to reveal the reaction mechanism during the self-propagating high-temperature synthesis (SHS) of Ti_3SiC_2 from furnace-ignited stoichiometric 3Ti + SiC + C mixtures. The diffraction patterns indicate that the SHS proceeded in five stages: (i) preheating of the reactants, (ii) the $\alpha \rightarrow \beta$ phase transformation in Ti, (iii) preignition reactions, (iv) the formation of a single solid intermediate phase in <0.9 s, and (v) the rapid nucleation and growth of the product phase Ti_3SiC_2. No amorphous contribution to the diffraction patterns from a liquid phase was detected and, as such, it is unlikely that a liquid phase plays a major role in this SHS reaction. The intermediate phase is believed to be a solid solution of Si in TiC such that the overall stoichiometry is ~3Ti:1Si:2C. Lattice parameters and known thermal expansion data were used to estimate the ignition temperature at 923 ± 10°C (supported by the $\alpha \rightarrow \beta$ phase transformation in Ti) and the combustion temperature at 2320 ± 50°C.**

I. Introduction

TITANIUM SILICON CARBIDE (Ti_3SiC_2) has attracted considerable interest in the literature because of a unique combination of physical properties.[1–23] These include a high melting point, good high-temperature strength, resistance to corrosion and oxidation, high Young's modulus, and high electrical/thermal conductivity—characteristics, which are both metallic and ceramic in nature.[1,2] Lateral force microscopy measurements indicate exceptionally low friction coefficients on cleavage faces;[3] however, the bulk friction coefficients are more akin to those of other ceramics.[4] Recent measurements have also revealed that the material has negligible thermoelectric power between 300 and 800 K.[5]

Ti_3SiC_2 has a hexagonal crystal structure consisting of double layers of TiC octahedra separated by a planar Si layer. The structure has space group $P6_3/mmc$ with lattice parameters a = 3.0675 Å, c = 17.6570 Å.[6,7] Recent band structure calculations indicate that ionic, covalent, and metallic bonds coexist within the structure.[8] This combination of properties and crystal chemistry has led to many interesting applications for the material being postulated. Potential applications include machinable structural ceramics that are corrosion, creep, and oxidation resistant; corrosion- and oxidation-resistant barrier coatings; intermediate phases in metal–ceramic bonding; electrodes in electrochemical cells (e.g., in aluminum smelting);[1,2] and conducting films on dielectric and semiconductor devices.[9,10] The primary difficulty in realizing these diverse applications is that, in common with all ternary or higher-order phases, it has proved difficult to synthesize Ti_3SiC_2 without unwanted "impurity" phases. The properties of these impurity phases (e.g., TiC_x and Ti_xSi_y type) are very different from those of Ti_3SiC_2; hence the properties of the final ceramic are strongly influenced by their presence.

Samples of Ti_3SiC_2 have been produced using many alternative methods. The first recorded synthesis of Ti_3SiC_2 was by reaction between TiH_2, Si, and graphite at 2000°C.[6] In that pioneering study, the Ti_3SiC_2 was present only as a minor impurity phase and was accompanied by considerable quantities of TiC_x and $Ti_5Si_3C_x$. Improvements in phase purity were achieved using chemical vapor deposition (CVD) with $SiCl_4$, $TiCl_4$, CCl_4, and H_2 as source gases.[11] Although 100% Ti_3SiC_2 was produced, the sample size was limited (40 mm × 12 mm × 0.4 mm) and the production rate was slow (200 μm/h)[11] compared with bulk techniques. Sample size has been increased using two alternative methods; reactive hot-pressing[1] and self-propagating high-temperature synthesis (SHS).[12–16] Barsoum *et al.*[1,2,17,18] have used reactive sintering and hot isostatic pressing (40 MPa for 4 h, at 1450°C) of 3Ti/SiC/C or $3TiH_2$/SiC/C pellets to produce high-purity Ti_3SiC_2 samples (>98%). The samples consisted of a fully dense ceramic body with uniform ≤5 μm grains. This treatment is hereafter referred to as reactive sintering or the conventional synthesis. Many of the properties of the ceramic have been measured on samples of this kind.

Although Barsoum *et al.* have achieved the greatest purity and density for Ti_3SiC_2 samples to date, the reactive sintering/hot isostatic pressing process is costly and difficult to scale up. Several forms of the alternative technique, SHS, have been developed for synthesizing Ti_3SiC_2.[12–16] SHS processing has perceived economies and advantages that have attracted considerable interest. These include the following: (i) the heat of reaction provides some or all of the thermal energy required for the process; (ii) the reaction times are very short; (iii) industrial scale-up is regarded as simpler. The earliest work, by Pampuch *et al.*,[19] used elemental powders of 3Ti/Si/2C, cold-pressed and heated to 1050–1200°C at a heating rate of 500 K/min. The material produced was up to 90% phase pure and reached a combustion temperature estimated at 1830°C. TiC was the major impurity phase with additional minor silicide phases. Later work by the same group has centered on purifying and densifying SHS-generated starting materials. Goesmann *et al.* developed an ultra-high-vacuum (UHV) electron-beam ignition technique using mixed Ti/SiC powders.[13] The powders were weighed to have a Ti:C molar ratio the same as Ti_3SiC_2 and a postreaction evaporation technique was used to remove the excess silicon. Samples with >92% Ti_3SiC_2 with minor amounts of TiC and $TiSi_2$ were fabricated. The ignition temperature was reported to be ~900°C, and the combustion temperature was estimated to be in the range 1700–2617°C. Postreaction heating

A. H. Carim—contributing editor

Manuscript No. 187376. Received October 24, 2001; approved June 22, 2002.

with an electron beam was conducted at 1500–1600°C for ~5 min to drive off excess Si. An average weight loss of 4% was solely attributed to silicon vaporization. Feng *et al.* incorporated *in situ* consolidation at 34.4 MPa during dc resistive heating ignited SHS of Ti_3SiC_2.[14] SHS combustion temperatures were shown to be dependent on the magnitude of an externally applied ac electric field at either 2260°C (0 V) or 2420°C (6.67 V). Similarly, the percentage of the TiC impurity phase was also very sensitive to the processing conditions. By far the greatest conversion was the >98% attained for samples held at 1525°C for 2 h after SHS ignition.[14] This latter method must be considered a hybrid of SHS and the conventional synthesis method.

Against the advantages of SHS must be balanced two major difficulties: (i) the products are usually very porous; (ii) to date, it has proved difficult to produce very high purity Ti_3SiC_2 in this way, other than by the hybrid method.[14]

To optimize an SHS method and minimize the formation of unwanted phases it is important to understand the mechanisms that control the growth of Ti_3SiC_2 as a product phase. The great speed of SHS reactions and the very high temperatures involved have caused the mechanisms to be poorly understood because sample characterization has relied on postreaction techniques[1,13,17,19,20] Often the physical characteristics of the microstructure have been used to postulate mechanisms that rely on the melting, either of one of the reactants[20] or of an intermediate phase such as TiC,[21] or titanium silicides.[22]

A mechanism for Ti_3SiC_2 formation during the reactive sintering of 3Ti/SiC/C mixtures was developed by these *ex situ* methods.[16,17] The proposed mechanism involved two intermediate phases, TiC and Ti_5Si_3, which form early in the sintering process and are later consumed in the formation of the final phase, Ti_3SiC_2.[17] Recent *in situ* neutron diffraction studies by the authors of this paper have confirmed the role of the intermediate phases TiC_x and $Ti_5Si_3C_x$ in the conventional synthesis and have shown that they are the only solid phases present over a wide range of temperature before the Ti_3SiC_2 product phase forms.[23,24] Postreaction XRD analyses of laboratory-generated SHS samples show residual TiC_x and small amounts of $Ti_5Si_3C_x$.[25] This led to the working hypothesis that the reaction would proceed by the SHS formation of the same intermediate phases, TiC_x and $Ti_5Si_3C_x$, followed by their post-SHS interaction to form Ti_3SiC_2.

To test this hypothesis, it was necessary to find a suitable *in situ* technique, as the *in situ* observation of Ti_3SiC_2 formation by SHS has not been previously attempted. *In situ* observations of SHS reactions have been successfully performed on several systems using X-ray diffraction.[26–36] These studies no doubt provided some valuable insight into the systems studied; however, some aspects were suboptimal. First, the systems chosen for study have been largely binaries where intermediate phases are unlikely to form and the reaction kinetics are extremely fast. Second, generally only a small angular range (as little as 6° 2θ, 38° 2θ at best) has been accessible, restricting the amount of structural and compositional detail that can be extracted from the diffraction patterns. Finally, of particular relevance to this work, the X-rays used are heavily absorbed by the sample, usually within 3–10 μm of the surface. SHS reactions are widely known to cause volatilization of some chemical species due to the high reaction temperatures. In the Ti–Si–C system, the major losses are thought to be Si,[1,37] which is supported by the successful electron beam evaporation of Si discussed above.[13] It is therefore unclear whether the surface of the sample would be truly representative of the bulk in the Ti–Si–C system. To overcome these shortcomings, we have used an ultra-high-speed *in situ* neutron diffraction instrument, D20 at the Institut Laue-Langevin, to study the SHS reaction of 3Ti/SiC/C mixtures. Neutrons are only weakly absorbed by this material and the diffraction pattern is therefore representative of the entire sample. Our results reveal an entirely new reaction mechanism.

II. Experimental Procedure

Stoichiometric 3Ti:1Si:2C powder mixtures of Ti powder (Sigma-Aldrich, −325 mesh, 99.98%), SiC powder (Performance Ceramics Japan, <100 μm, 99.9%), and graphite powder (Aldrich, <100 μm, 99.9%) were mixed by hand in a mortar and pestle under an argon atmosphere (<5 ppm O_2, <10 ppm H_2O). A schematic diagram of the sample environment is shown in Fig. 1. Each sample was comprised of two or three 6-g pellets, 12.2 mm high and 15.2 mm in diameter, prepared by cold-pressing at 180 MPa in a steel die. The pellets were stacked and placed at the center of a 16 mm inner diameter (ID) silica (SiO_2) tube with a wall thickness of 1.5 mm. An insulating section of Al_2O_3 was placed atop a stainless steel support stand with a 3 mm thick Ti disk separating the sample from the ceramic. Primary heating, ignition, and neutron diffraction data collection were all conducted in a resistive vanadium vacuum furnace operating under a pressure of $\sim 10^{-2}$ mbar. The sample and the silica tube were placed at the center of an interchangeable (V or Nb), 20 mm ID heating element (20–40 μm thick). A boron carbide (B_4C) mask positioned 3200 mm from the main reactor aperture and 50 mm from the sample focal plane limited the neutron beam height to 42 mm with a divergence of 3 mm. Care was taken to ensure that the support stand, the Ti disk, and the Al_2O_3 section were well outside the penumbra of the neutron beam. K-type thermocouples were positioned ~3 mm below the base of the Ti disk and used to control the furnace temperature. These also provided a rudimentary means to monitor the exothermic ignition of the sample. Neutron diffraction patterns were recorded in transmission geometry on the D20 diffractometer at the Institut Max von Laue-Paul Langevin, Grenoble, France, using a neutron wavelength of 1.3008 ± 0.0001Å. The instrument is equipped with a microstrip position sensitive detector allowing simultaneous detection of diffraction patterns in the range 10–150° 2θ in arbitrarily short times down to 30 μs (limited only by the diffracted intensity from the sample).

A high-intensity diffraction pattern was recorded at room temperature from each starting mixture. Samples were then preheated from room temperature to 400°C at 30°C/min. Between 400° and 850°C the heating rate was maintained at 30°C/min. During this temperature interval, neutron diffraction patterns were collected for 5 s each with an average data transfer time of 1 s. From 850° to 1050°C the heating rate was increased, initially to 102°C/min and decreasing progressively to ~8°–15°C/min at 1000°C for the V heating element. During the same temperature

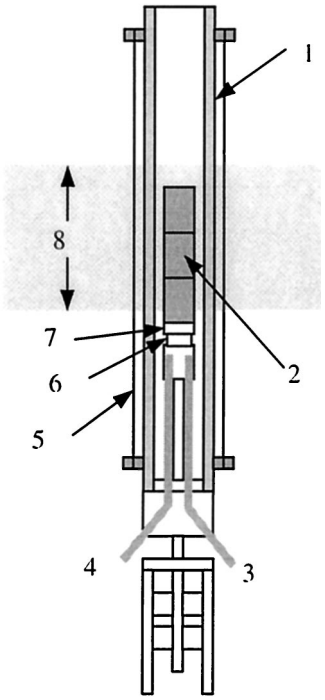

Fig. 1. Schematic diagram of the experimental arrangement: (1) protective silica tube, (2) sample pellets, (3,4) furnace control thermocouples, (5) metal foil heating element (V or Nb), (6) insulating Al_2O_3 disk, (7) Ti disk, and (8) the neutron beam height.

interval, the data acquisition time was decreased to 0.9 s including 0.4 s for data transfer (i.e., patterns were recorded in 0.5 s). SHS ignition and combustion reactions occurred toward the latter part of this interval. Data collection was terminated ~15–20 min after ignition of the self-propagating reaction. Two samples were studied in the experimental arrangement shown in Fig. 1 and a third was studied without the intermediate SiO_2 tube and using a Nb furnace element instead of V. Results from the three samples are very similar and differ only in some minor details that will be highlighted in the appropriate sections to follow.

Reaction products were examined using optical microscopy, SEM, and XRD (Cu$K\alpha$). Diffraction patterns were analyzed using the Rietveld analysis program FULLPROF.[38] Refined parameters for major phases were typically a zero correction, scale factors, peak shape parameters, atomic occupancies, and lattice parameters. An interpolated fixed background was used to account for the presence of amorphous scattering from the silica tubing. This profile was obtained from the room-temperature reactant pattern with minor modifications for the influence of increasing temperature. Visual analysis of phase transformations and the reaction mechanism were obtained using the large array manipulation program (LAMP).[39]

III. Results

(1) Reaction Overview

Because of the excellent time resolution of the experiment (0.5 s to record each diffraction pattern and 0.4 s for data download), an enormous amount of detail is apparent in the resulting diffraction patterns. A comprehensive overview of the time evolution of the experiment is given by composite diagrams

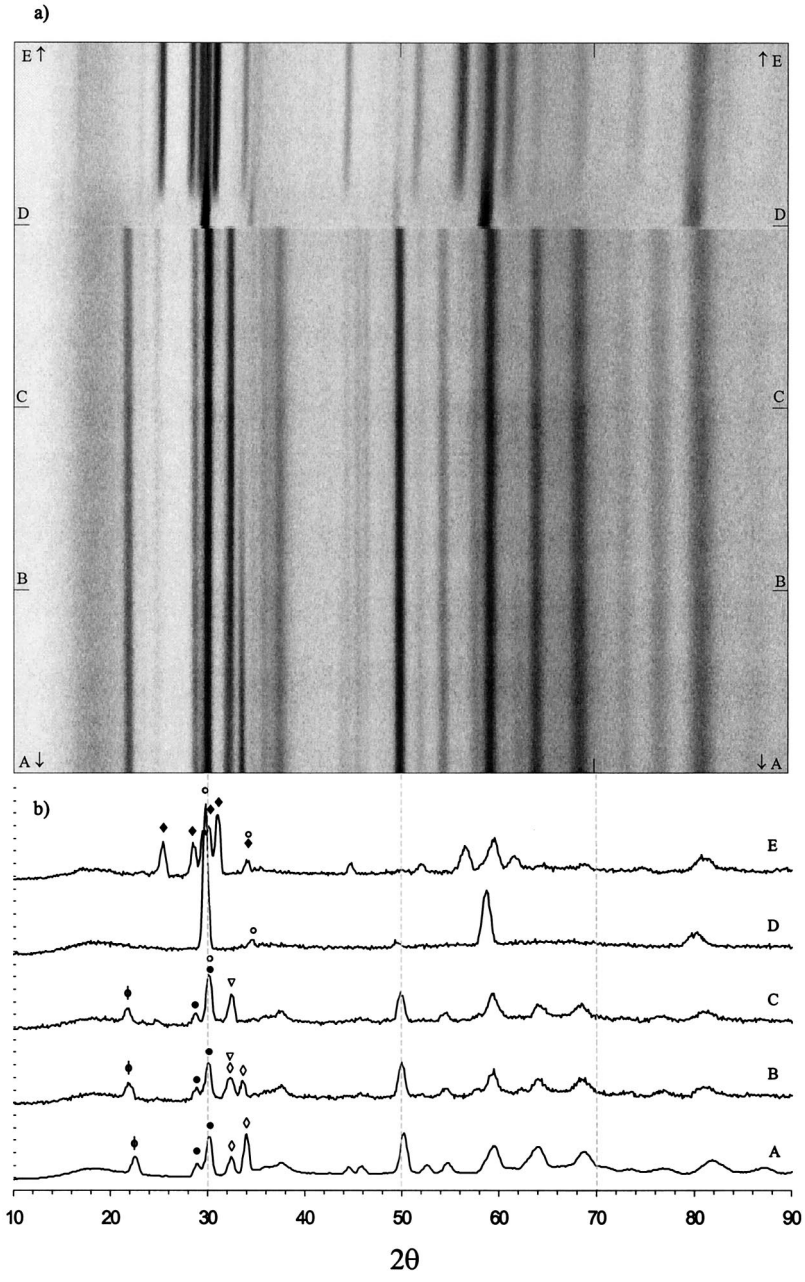

Fig. 2. (a) Representation of part of the diffraction patterns collected from the second sample. The *x*-axis is the diffraction angle 2θ, the *y*-axis is time (at 0.9 s per diffraction pattern), and the brightness is the diffracted neutron intensity. All five stages of the reaction are represented here. Most dramatic is the discontinuity created by the SHS reaction. (b) Selected diffraction patterns to represent the five stages of the reaction (preheating of the reactants, the $\alpha \rightarrow \beta$ phase transformation in Ti, preignition reactions, an intermediate phase, and the growth of the product phase). Reflections characteristic of each phase are marked as follows: (ϕ) C, (●) SiC, (◇) α-Ti, (○) TiC_x, (▽) β-Ti, (◆) Ti_3SiC_2.

such as that shown in Fig. 2(a). In Fig. 2(a), time is shown on the vertical axis and the diffraction angle (2θ) on the horizontal axis. Increased brightness indicates increased diffracted intensity on a third axis perpendicular to the page. Five distinct stages were identified. These are represented by the selected diffraction patterns A–E in Fig. 2(b), which is plotted on the same 2θ scale as Fig. 2(a). These respectively represent (A) the initial reactants, (B) the start of the α-Ti → β-Ti transformation, (C) a preignition stage between the completion of the α-Ti → β-Ti transformation and the ignition event, (D) the rapid evolution of an intermediate phase, and (E) the formation of the product phase, Ti_3SiC_2. These stages will be discussed in turn in the sections that follow.

(2) Stage 1, Initial Reactants

The diffraction pattern of each sample at room temperature consists of the reactant powders—α-Ti, SiC, and graphite—as represented by pattern A in Fig. 2(b). The presence of an amorphous background (e.g., at 14–22° 2θ) is attributable to the silica tubing surrounding the sample. This was readily accounted for in the Rietveld analysis via a fixed background. Below a furnace temperature of 906 ± 10°C the neutron diffraction patterns show only the expected thermal expansion of the reactant phases. The thermal expansion allows an estimate of the sample temperature at any stage of the reaction, to be made based on the lattice expansion and known thermal expansion data.

(3) Stage 2, α-Ti → β-Ti Transformation

The transformation of α-Ti to the β polymorph is the first significant change in the samples. It is most easily observed by the decrease in the intensity of the diffraction peak near 34° and the corresponding increase in the intensity of the peak at 32.2°. A representative diffraction pattern is shown as pattern B of Fig. 2(b). For this pattern, the integrated intensities indicate ~50% completion of the transformation. Using the thermal expansion of the reactants to calculate the temperature of the sample, it was estimated that the α-Ti → β-Ti transformation began at 901 ± 8°C in good agreement with the literature value of 882°C for pure Ti and 920°C at the C solubility limit. The complete α-Ti → β-Ti transformation occurs over a furnace temperature interval of 69C°. During the same time interval, the average sample temperature, estimated from the thermal expansion of the SiC reactant, changed by only 22°C. We believe this smearing out of the transformation to be due to a temperature gradient from the surface to the center of the sample. The transformation rate is hence controlled by the thermal conductivity of the pellet. Other than this obvious phase transformation, there are no significant changes in the phase composition of the samples before the completion of the α-Ti → β-Ti transformation.

(4) Stage 3, Preignition

Between the end of the α-Ti → β-Ti transformation and the SHS ignition, over a period of approximately 1 min, there are small but significant changes to the diffraction patterns. Careful comparison of patterns B and C in Fig. 2(b) reveal an increase in the intensity of the peak near 30°. This peak is the major reflection from SiC; however, it overlaps with TiC. There is an associated decrease in the intensity of the β-Ti reflections (e.g., at 32.2°). The changes are more clearly seen in Fig. 3, a three-dimensional rendering of part of Fig. 2(a). Analysis of the complete diffraction patterns in this region using Rietveld refinements confirms the growth of a TiC_x phase at the expense of β-Ti and free carbon. By the time of the SHS ignition, there is 11 ± 2 wt% TiC_x in the sample and the rate of formation is accelerating as indicated by the integrated intensities of the composite SiC/TiC reflection at 30°, shown in Fig. 4. Close scrutiny of the diffraction patterns immediately before ignition suggests that a very small amount of $Ti_5Si_3C_x$ is present. These phase quantities are in agreement with earlier postreaction XRD analyses.[25]

(5) Stage 4, Intermediate Phase

The SHS ignition event is readily seen in Figs. 2(a) and 3 as a complete discontinuity in the diffraction signal. A closer view of the ignition event is shown in Fig. 5 for one of the samples. In less than 0.9 s, the reactant diffraction patterns were replaced by patterns like pattern D in Fig. 2(b). The entire 20 g samples had apparently converted to a single solid phase with a NaCl structure not unlike TiC. This was confirmed by Rietveld analyses such as the one shown in Fig. 6. The intermediate phase is believed to be a Si-substituted TiC with approximately the same stoichiometry as the overall sample. The structure and significance of the intermediate phase will be discussed in Section IV(3).

The intermediate phase persisted as the only solid phase for 6 s[†] after the ignition event before nucleation and growth of the product phase began. An estimate of the sample temperature during and following SHS ignition was made using the lattice contraction of the intermediate phase on cooling. The lattice parameter at the end

[†]In the sample without the SiO_2 tube this time was reduced to 4 s.

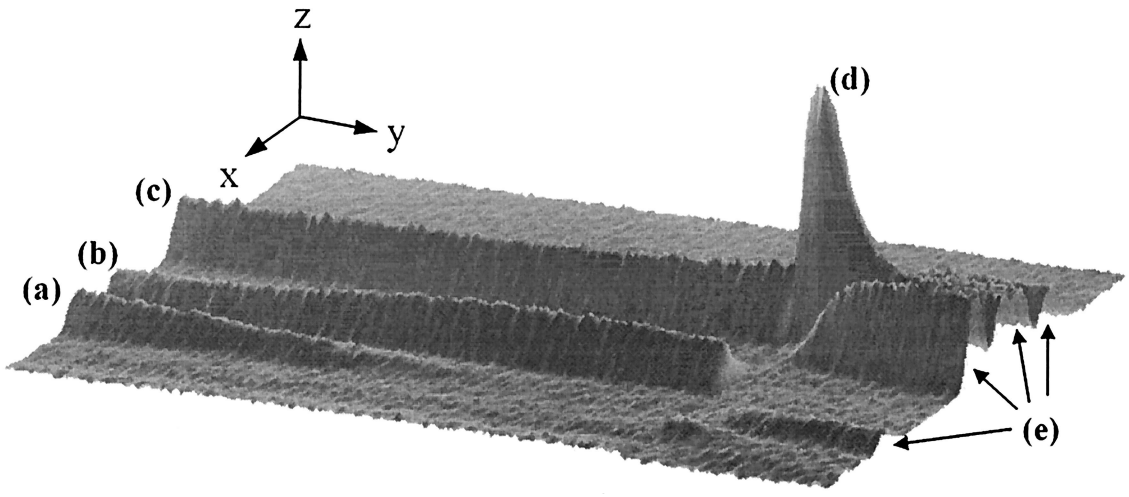

Fig. 3. Three-dimensional rendering of part of Fig. 2(a) to highlight reaction stages 2–5. The diffraction angle 2θ in the range 26–36° lies along the *x*-axis, time lies along the *y*-axis, and the diffracted intensity is shown along the *z*-axis. The letters indicate identifying diffraction peaks from (a) α-Ti, (b) initially α-Ti, later becoming β-Ti, (c) initially SiC but overlapped by some TiC in the approach to ignition, (d) the intermediate TiC-like phase, and (e) the Ti_3SiC_2 product phase.

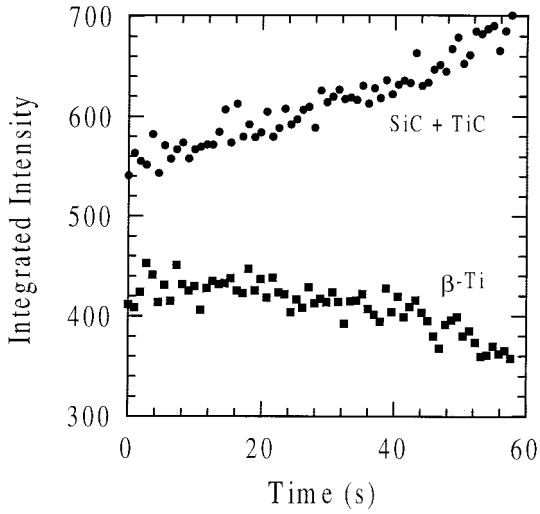

Fig. 4. Integrated intensity of the reflections near 30° and 32.2° 2è. The upper reflection is a composite of the (006) and (102) reflections of SiC, and the (200) reflection from TiC_x. The lower reflection is (110) from β-Ti. The accelerating rate of TiC formation just before SHS ignition is obvious.

of the experiment was used as a reference on the assumption that the sample had cooled to be at the known furnace temperature. The thermal expansion coefficient used is that for pure TiC[40] and may be slightly in error due to Si substitution. The resulting temperature profile is shown in Fig. 7, illustrating a maximum estimated at 2597 K. The temperature had decreased to ~2350 K before the Ti_3SiC_2 product phase was observed in the diffraction patterns.

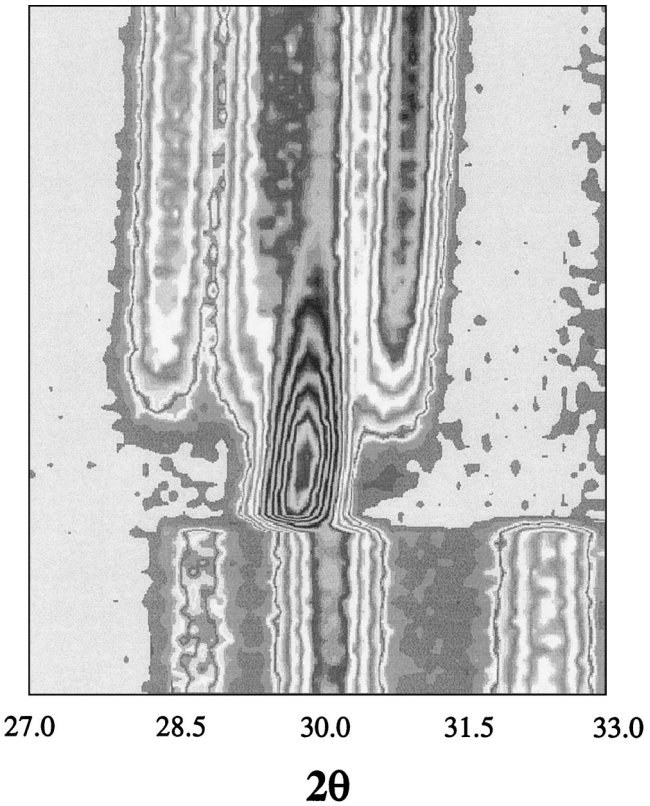

Fig. 5. Close-up view of neutron diffraction data recorded during the SHS ignition, incubation time, and growth of the product phase. Note the curvature due to thermal contraction of the products which allows the sample temperature to be estimated.

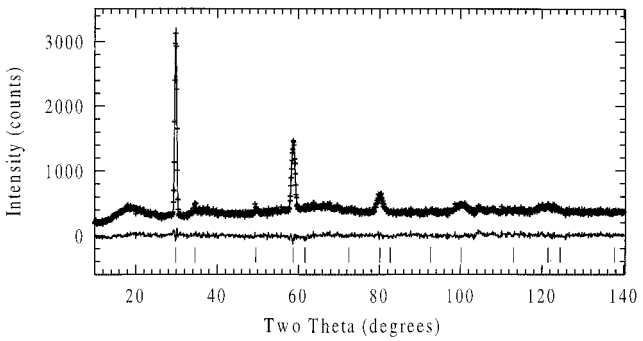

Fig. 6. Results of the Rietveld refinement of the intermediate phase structure. The data are shown as "+", the calculation and difference profiles as solid lines, and reflection markers as vertical bars below the figure.

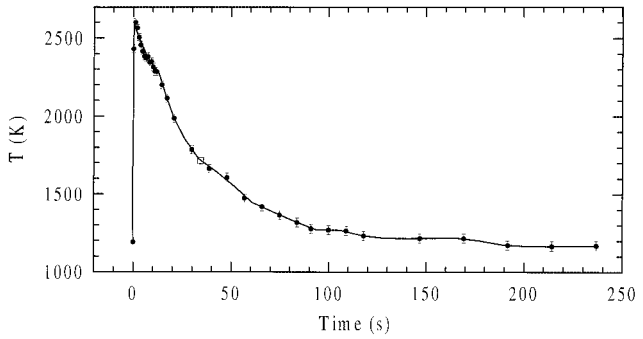

Fig. 7. Sample temperature as a function of time beginning with the SHS ignition. The beginning of Ti_3SiC_2 precipitation is obvious as a marked change of slope at 2350 K. The end of the Ti_3SiC_2 formation is marked in the figure by an open square symbol.

(6) Stage 5, Product Phase Formation

After the 6-s incubation time, the product phase Ti_3SiC_2 begins to appear in the diffraction patterns at the upper end of Figs. 2(a) and 5. The rate of growth is quite rapid and is more clearly seen in Fig. 3. After only a further 35 s, 80 wt% of the sample has converted to the product phase and there is little further growth of product phase thereafter. The sample temperature at this time is estimated to have been 1723 K. The amount of intermediate phase remaining at the end of the reaction is greater than the amount of TiC_x formed in the preignition stage and we are unable to conclude anything concerning the fate of the TiC_x.

IV. Discussion

(1) Preignition

The ignition temperatures reported for SHS reactions in the Ti–Si–C system vary widely.[19,21] Potentially, this may depend on the starting materials, the powder pretreatment, or the heating rate used. It is not always clear whether it is the sample temperature or the furnace temperature at ignition that has been reported. In this work, the furnace temperature at ignition was 988°, 1015°, and 1008°C for samples with terminal heating rates of 15°, 8°, and 100°C/min, respectively, the latter using the Nb heating element. In these experiments, the diffraction data give us two additional independent measures of the sample temperature: the thermal expansion of the starting materials and the $\alpha \rightarrow \beta$ transition in Ti. In all cases, the $\alpha \rightarrow \beta$ transition was complete before ignition, meaning that the ignition temperatures were greater than 882°–920°C (depending on the amount of C in solid solution in the Ti). Estimates using the lattice expansion give ignition temperatures of 923 ± 10°C in samples with an estimated thermal gradient of 22°C.

It has been noted in previous *in situ* neutron diffraction work on the conventional synthesis of Ti_3SiC_2[23,24] that the $\alpha \rightarrow \beta$ phase transition is generally observed to occur before the formation of detectable amounts of the critical intermediate phases TiC_x and $Ti_5Si_3C_x$. This is also the case for all three samples studied in the work reported here. It would appear that the β phase reactivity is significantly higher than that of the α phase.

Once the $\alpha \rightarrow \beta$ transformation is complete, signs of TiC are very rapidly seen in the diffraction patterns as shown, for example, in Fig. 5. TiC formation is highly exothermic and is believed to provide additional energy to make the reaction self-sustaining. As with all SHS reactions, the rate of heat generated by the reaction needs to exceed the rate of heat loss to the surroundings. Once this condition is attained, the system is essentially in a state of undamped positive feedback and the reaction goes quickly to completion. As such we see in Fig. 5, rapid growth in the rate of the reaction $Ti + C \rightarrow TiC$ up to the point of SHS ignition.

With the starting materials used in this work, $3Ti + SiC + C$, there is a further criterion to be met, namely that the system locally attain a high enough temperature (via the reaction of the limited amount of free C with Ti) for Ti to rapidly react with SiC to release Si (of order 1200–1400°C in diffusion couples[9,13,41]). Thus the critical heat release rate for SHS must be attained before the free C is consumed or else the SHS will not initiate.

(2) Liquid-Phase Formation

It has been widely hypothesized in the literature that many SHS reactions involve a liquid phase[42] and this idea has been widely accepted. The parameters governing the formation of a liquid are thought to be the particle size and combustion temperature. Larger particles and higher combustion temperatures both promote liquid formation whereas fine particles are thought to react in the solid state. In the Ti–Si–C system, evidence of liquid-phase formation has been in the form of postreaction surface microstructures that appear to have been molten and some continuum heat-flow modeling.[20–22] In the current work, the presence of a substantial amount of a liquid phase would give rise to an amorphous background contribution in the diffraction patterns. Unfortunately, data for our first two samples already have an amorphous background due to the SiO_2 tube. Detailed background comparisons between diffraction patterns collected just before and just after the SHS ignition do not reveal any significant differences other than those due to temperature increase. In addition, the third sample has no SiO_2 background and again no amorphous scattering was detected. It is difficult to place a detection limit on these remarks; however, based on the intensity of the SiO_2 patterns and the amount of SiO_2 in the neutron beam, it is estimated to lie in the 2–4 wt% range. To improve the counting statistics, the six patterns collected during the incubation period just before the precipitation of the product phase were summed and subjected to a similar scrutiny of the background. Again no additional amorphous scattering was found. These observations do not rule out the formation of small amounts of an interfacial liquid.

If large amounts of liquid did form, it did so in less than 0.4 s and the intermediate phase precipitated from it within that time. Even if this is what occurred, the major part of the reaction path is as observed via the neutron diffraction—a single solid intermediate (TiC-like) phase leading to the product phase Ti_3SiC_2.

(3) Intermediate Phase

Based on the work of El-Raghy *et al.*[17,18] and our own low-time-resolution *in situ* neutron diffraction studies of Ti_3SiC_2 synthesis from Ti/SiC/C starting mixtures,[23–25] it was expected that the intermediate phases TiC_x and $Ti_5Si_3C_x$ would play an important role in the SHS reaction. Indeed, some TiC was formed in the preignition stage of the reaction and very minute amounts of $Ti_5Si_3C_x$ were detected in stages 3–5 of the reaction. However, in all three samples, stage 3 was dominated by a single intermediate phase isostructural with TiC. In the absence of any compelling evidence for a liquid phase, the absence of any other solid phases and no evidence for the loss of most of the Si by evaporation,[‡] the intermediate phase is considered to be a solid solution of Si in TiC. Depending on which crystallographic site is occupied by the Si, the phase could be either $(Ti_{0.75}Si_{0.25})C_{0.5}$ or $Ti(Si_{0.33}C_{0.66})$ assuming the same stoichiometry as the starting mixture.

Confirming the nature of the intermediate phase has proved difficult. If it could be assumed that both crystallographic sites in the structure were fully occupied, the refinement of site occupancies during Rietveld analysis would allow identification of the site occupied by the Si. Unfortunately, TiC_x can take values of x between 0.6 and 1.0 on the standard Ti–C phase diagram.[43] The situation is most readily illustrated by examining the structure factors for the NaCl structure type:

$$F^2 = 16(b_A + b_B)^2 \qquad ((h + k + l) \text{ even}) \tag{1a}$$

$$F^2 = 16(b_A - b_B)^2 \qquad ((h + k + l) \text{ odd}) \tag{1b}$$

where the b's are the neutron scattering lengths—analogous to the X-ray form factors in X-ray diffraction. The subscript A refers to the site occupied by Ti and B to the site occupied by C in TiC. The scattering lengths for the elements of interest here are -0.3438,[§] 0.41491, and 0.6646 for Ti, Si, and C, respectively, in units of 10^{-12} cm. Taking first the possibility that Si substitutes on the A site, the approximate formula would be $(Ti_{0.75}Si_{0.25})C_{0.5}$ and the structure factors would be as given in column 2 of Table I. On the other hand, if the Si substitutes on the B site forming $Ti(Si_{0.33}C_{0.66})$, the structure factors are given in column 3 of Table I. In a high-intensity diffraction pattern, these would be readily distinguishable from each other and from TiC although the distinction between $(Ti_{0.75}Si_{0.25})C_{0.5}$ and TiC is less well-defined. Unfortunately all of these compositions are merely members of a continuous spectrum of possible compositions and structure factors. Since standard structure refinement techniques give structural parameters based on the relative intensities of the two kinds of reflection, there is no unique solution.

A TiC-like cubic phase with dissolved Si has been proposed by Barsoum *et al.* to form during the attack of Ti_3SiC_2 by molten cryolite as a result of the egress of Si.[44] The formation mechanism proposed by those authors involves both the organized shear of *a–b* planes in the Ti_3SiC_2 and short-range diffusion of Si—essentially the reverse of that required to transform the cubic intermediate into Ti_3SiC_2. This process involves Si partitioning onto selected (111) planes of the TiC-like structure and should lead to superlattice reflections. Our diffraction patterns do not show definite superlattice reflections; however, given that only a small fraction of the sample may be in this partially ordered transition state, the intensity of the 0.5 s patterns is not sufficient to rule out this mechanism.

(4) Product Phase

The Ti_3SiC_2 product phase does not form directly from the self-propagating high-temperature synthesis reaction, but rather forms via the cubic intermediate phase. Ti_3SiC_2 precipitates directly from the intermediate phase in 35 s, after a short incubation period, as illustrated at the top of Fig. 5. It is difficult to determine whether the time lapse after the SHS and before precipitation of the Ti_3SiC_2 is a genuine incubation time, or merely

[‡]For example, the sample eventually converts into 80 wt% Ti_3SiC_2 and so the fraction of Si lost is at worst 20% and is believed to be much less.

[§]Ti scatters neutrons 180° out of phase with most other elements and is hence given a negative scattering length.

Table I. Illustrative Values of F^2

	F^2		
	$(Ti_{0.75}Si_{0.25})C_{0.5}$	$Ti(Si_{0.33}C_{0.66})$	TiC
$(h + k + l)$ even	0.5080	0.8594	1.6466
$(h + k + l)$ odd	3.7857	13.532	16.270

the time required for the sample temperature to fall to a critical value. The shorter incubation time for the third sample, without the SiO_2 shield, favors the latter explanation. The temperature at which Ti_3SiC_2 begins to precipitate in Fig. 7 is ~2350 K (2077°C), far higher than that used in the conventional synthesis. This is the highest temperature at which Ti_3SiC_2 has been observed by diffraction and its formation at this temperature contradicts claims that the phase is unstable at temperatures above 1400°C.[15,45] It can be noted from the deviation of the cooling curve in Fig. 7 that Ti_3SiC_2 precipitation is exothermic. This observation, using only diffraction-based thermometry, has led us to propose a new method for very high temperature DTA.[46] The cessation of Ti_3SiC_2 formation at 1723 K (1450°C) is in good agreement with literature observations that this is the minimum temperature for successful reactive sintering.[1,2,17,18,47,48]

As noted in Section IV(3), the primary difference between SHS and the conventional synthesis is that the latter involves two intermediate phases, TiC_x and $Ti_5Si_3C_x$.[17,18,23,24] Further differences can be identified by considering the atom migration involved in the production of the Ti_3SiC_2 phase. In the conventional synthesis, distinct crystals of the two intermediate phases need to decompose and their constituent atoms migrate over distances commensurate with the crystallite dimensions—of order 1–5 μm. *In situ* neutron diffraction studies have shown that this process takes ~20 min at 1500°C to reach the same state of completion as the samples used here. In the mechanism observed here, the Ti, Si, and C atoms are already well mixed within the intermediate phase and only short-ranged atom migration on the scale of individual unit cells is required.

V. Conclusions

This experiment has demonstrated the power of *in situ* neutron diffraction to reveal the reaction mechanisms, structural details, and microstructural evolution of complex multicomponent systems. It has allowed the following conclusions to be drawn:

(1) Self-propagating high-temperature synthesis is readily initiated in 3Ti/SiC/C mixtures by a simple furnace ignition at initial heating rates of 100°C/min.

(2) Conversion to the desired product phase was ~80 wt% during the *in situ* experiment without any attempt to optimize the process.

(3) The reaction proceeds via five stages: preheating of the reactants, the $\alpha \rightarrow \beta$ phase transformation in Ti, preignition reactions, an intermediate phase, and the growth of the product phase.

(4) Stage 2, the allotropic $\alpha \rightarrow \beta$ phase transformation in Ti appears to trigger the SHS reaction. We have postulated that this is due to higher reactivity of the β phase.

(5) Stage 3, the reaction of Ti with free carbon in the starting mixture to form TiC_x provides the initial energy, above that provided by the furnace, required to initiate the SHS.

(6) SHS occurs very rapidly, converting the entire sample into a cubic intermediate phase in 0.5 s or less. The combustion temperature was estimated at 2597 K from the thermal contraction of the intermediate and product phases.

(7) There are no signs of a substantial amount of a liquid phase in the reaction. If such a phase forms, it either forms in small quantities (possibly as an interfacial liquid) or forms and solidifies very rapidly (less than 0.4 s).

(8) The intermediate cubic phase is most likely a solid solution of Si in TiC.

(9) Ti_3SiC_2 precipitates and grows from the intermediate phase in ~35 s after an incubation time of ~6 s.

Acknowledgments

We wish to thank the staff of the Institut Laue-Langevin, without whose help this experiment would not have been a success. We wish to thank in particular Pierre Convert, Gwenaelle Rousse, and Jacques Torregossa.

References

[1]M. W. Barsoum and T. El-Raghy, "Synthesis and Characterization of a Remarkable Ceramic: Ti_3SiC_2," *J. Am. Ceram. Soc.*, **79**, 1953–56 (1996).

[2]M. W. Barsoum and T. El-Raghy, "A Progress Report on Ti_3SiC_2, Ti_3GeC_2, and the H-phases, M2BX," *J. Mater. Synth. Process.*, **5** [3] 197–216 (1997).

[3]S. Myhra, J. W. B. Summers, and E. H. Kisi, "Ti_3SiC_2—A Layered Ceramic Exhibiting Ultra-Low Friction," *Mater. Lett.*, **39**, 6–11 (1999).

[4]T. El-Raghy, P. Blau, and M. W. Barsoum, "Effect of Grain Size on Friction and Wear Behaviour of Ti_3SiC_2," *Wear*, **238**, 125–30 (2000).

[5]H. I. Yoo, M. W. Barsoum, and T. El-Raghy, "Ti_3SiC_2 Has Negligible Thermopower," *Nature (London)*, **407** [6804] 581–82 (2000).

[6]W. Jeitschko and H. Nowotny, "Diffraction Thermometry and Differential Thermal Analysis," *Monatasch. Chem.*, **98**, 329–37 (1966).

[7]E. H. Kisi, J. A. A. Crossley, S. Myhra, and M. W. Barsoum, "Structure and Crystal Chemistry of Ti_3SiC_2," *J. Phys. Chem. Solids*, **59**, 1437–43 (1998).

[8]N. Medvedeva, D. Novikova, A. Ivanovsky, M. Kuznetsov, and A. Freeman, "Electronic Properties of Ti_3SiC_2-Based Solid Solutions," *Phys. Rev. B*, **58**, 16042–50 (1998).

[9]M. Witthaut, R. Weiss, E. Zimmerman, A. von Richthofen, and D. Neuschuetz, "Formation of Interface Phases in the Diffusion Couple of Ti–SiC," *Mater. Res. Adv. Technol.*, **89** [9] 623–28 (1998).

[10]F. Goesmann and R. Schmid-Fetzer, "Metals on 6H-SiC: Contact Formation from the Materials Science Point of View," *Mater. Sci. Eng.*, **B46**, 357–62 (1997).

[11]T. Goto and T. Hirai, "Chemically Vapour Deposited Ti_3SiC_2," *Mater. Res. Bull.*, **22**, 1195–201 (1987).

[12]R. Pampuch, J. Lis, J. Piekarczyk, and L. Stobierski, "Ti_3SiC_2-Based Materials Produced by Self-Propagating High-Temperature Synthesis (SHS) and Ceramic Processing," *J. Mater. Synth. Proc.*, **1** [2] 93–100 (1993).

[13]F. Goesmann, R. Wenzel, and R. Schmid-Fetzer, "Preparation of Ti_3SiC_2 by Electron-Beam-Ignitied Solid-State Reaction," *J. Am. Ceram. Soc.*, **81** [11] 3025–28 (1998).

[14]A. Feng, T. Orling, and Z. A. Munir, "Field-Activated Pressure-Assisted Combustion Synthesis of Polycrystalline Ti_3SiC_2," *J. Mater. Res.*, **14** [3] 925–39 (1998).

[15]P. Komarenko and D. E. Clarke, "Synthesis of Ti_3SiC_2-Based Materials Using Microwave-Initiated SHS," *Ceram. Eng. Sci. Proc.*, **15** [5] 1028–35 (1994).

[16]R. Radhakrishnan, S. B. Bhaduri, and C. H. Henager, "Analysis on the Sequence of Formation of Ti_3SiC_2 and Ti_3SiC_2/SiC Composites," *Adv. Powder Metall. Part. Mater.*, **3** [13] 129–37 (1995).

[17]T. El-Raghy and M. W. Barsoum, "Processing and Mechanical Properties of Ti_3SiC_2: I, Reaction Path and Microstructure Evolution," *J. Am. Ceram. Soc.*, **82**, 2849–54 (1999).

[18]T. El-Raghy and M. W. Barsoum, "Processing and Mechanical Properties of Ti_3SiC_2: II, Effect of Grain Size and Deformation Temperature," *J. Am. Ceram. Soc.*, **82**, 2855–60 (1999).

[19]R. Pampuch, J. Lis, L. Stobierski, and M. Tymkiewicz, "Solid Combustion Synthesis of Ti_3SiC_2," *J. Eur. Ceram. Soc.*, **5**, 283–87 (1989).

[20]J. Lis, R. Pampuch, J. Piekarczyk, and L. Stobierski, "New Ceramics Based on Ti_3SiC_2," *Ceram. Int.*, **19**, 219–22 (1993).

[21]R. Pampuch, M. Raczka, and J. Lis, "The Role of Liquid Phase in Solid Combustion Synthesis of Ti_3SiC_2," *Int. J. Mater. Prod. Tech.*, **10**, 3–6 (1995).

[22]J. Lis, R. Pampuch, T. Rudnik, and Z. Wegrzyn, "Reaction Sintering Phenomena of Self-Propagating High-Temperature Synthesis-Derived Ceramic Powders in the Ti–Si–C System," *Solid State Ionics*, **101–103**, 59–64 (1997).

[23]E. Wu, E. H. Kisi, S. J. Kennedy, and A. J. Studer, "*In Situ* Neutron Powder Diffraction Study of Ti_3SiC_2 Synthesis," *J. Am. Ceram. Soc.*, **84** [11] 2281–88 (2001).

[24]E. Wu, E. H. Kisi, D. P. Riley, and R. I. Smith, "Intermediate Phases in Ti_3SiC_2 Synthesis from Ti/SiC/C Mixtures Studied by Time-Resolved Neutron Diffraction," unpublished work.

[25]E. H. Kisi, D. P. Riley, E. Wu, and A. McCallum, "Combustion Synthesis of Ti_3SiC_2 from 3Ti/SiC/C Observed Using Neutron Diffraction," *Mater. Lett.*, submitted.

[26]Ch. Gras, F. Charlot, E. Gaffet, F. Bernard, and J. C. Niepce, "*In Situ* Synchrotron Characterization of Mechanically Activated Self-Propagating High-Temperature Synthesis Applied in Mo–Si System," *Acta Mater.*, **47** [7] 2113–23 (1999).

[27]F. Charlot, E. Gaffet, F. Bernard, Ch. Gras, V. Mathae, D. Klein, and J. C. Niepce, "Mechanically Activated SHS Reaction in the Fe–Al System: *In Situ* Time Resolved Diffraction Using Synchrotron Radiation," *Mater. Sci. Forum*, **269–272**, 379 (1998).

[28]V. V. Boldyrev, V. V. Aleksandrov, M. A. Tolochko, M. A. Gusenko, A. S. Sokolov, M. A. Sheronov, and N. Z. Lyakhov, "Investigation of the Dynamics of Phase Formation during the Synthesis of Nickel Aluminide in Combustion Regime," *Combust., Explos. Shock Waves (Engl. Transl.)*, **259** [5] 722 (1981).

[29]J. Wong, E. M. Larson, J. B. Holt, P. A. Waide, B. Rupp, and R. Frahm, "Time Resolved Diffraction Study of Solid Combustion Reactions Using Synchrotron Radiation," *Science*, **249**, 1406 (1990).

[30]E. M. Larson, J. Wong, J. B. Holt, P. A. Waide, G. Nutt, B. Rupp, and L. J. Treminello, "A Time Resolved Diffraction Study of the Ta–C Solid Combustion System," *J. Mater. Res.*, **8** [7] 1533 (1993).

[31]V. Gauthier, F. Bernard, E. Gaffet, C. Josse, and J. P. Larpin, "*In Situ* Time Resolved X-ray Diffraction Study of the Formation of the Nanocrystalline $NbAl_3$ Phase by Mechanically Activated Self-Propagating High-Temperature Synthesis Reaction," *Mater. Sci. Eng.*, **A272**, 334–41 (1999).

[32]A. G. Merzhanov, I. P. Borovinskaya, V. I. Ponomarev, I. O. Khomeko, Y. V. Zanevskii, S. P. Chernenko, L. P. Smykov, and G. A. Cheremukhina, "Dynamic X-ray Diffraction of Phase Formation during Self-Propagating High-Temperature Synthesis," *Dokl. Akad. Nauk SSSR*, **328**, 72–74 (1992).

[33]J. F. Javel, M. Dirand, J. J. Kuntz, F. Z. Nazzik, and J. C. Gachon, "Real Time X-ray Difraction Study of the Formation by SHS of the Phases γ' and H in the Ternary System Al–Ni–Ti," *J. Alloys Compd*., **247**, 72 (1997).

[34]C. R. Kachelmeyer, I. O. Khomenko, A. S. Rogachev, and A. Varma, "A Time-Resolved X-ray Diffraction Study of Ti_5Si_3 Product Formation during Combustion Synthesis," *J. Mater. Res*., **12**, 3230 (1997).

[35]F. Charlot, F. Bernard, E. Gaffet, and J. C. Niepce, "In Situ Time-Resolved Diffraction Coupled with a Thermal IR Camera to Study Mechanically Activated SHS Reaction: Case of Fe–Al Binary System," *Acta Mater*., **47** [2] 619 (1999).

[36]Ch. Gras, E. Gaffet, F. Bernard, and J. C. Niepce, "Enhancement of Self-Sustaining Reaction by Mechanical Activation: Case of an Fe–Si System," *Mater. Sci. Eng. A*, in press.

[37]N. Ya, V. S. Bilnovskov, D. G. Gorshkov, I. G. Grigorov, V. A. Perleyaev, and G. P. Shveikin; p. 351 in Proceedings of the 4th Euroceramics, C.N.R.–IRTEC (Faenza, Italy, 1995).

[38]J. Rodriguez-Carvajal, "FULLPROF Rietveld Analysis Software," Laboratoire Leon Brillouin (CEA-CNRS) France, ftp://charybde.saclay.cea.fr/pub/divers/fullprof.98/.

[39]D. Richard, M. Ferrand, and G. J. Kearley, "Large Array Manipulation Program (LAMP)," Institut Laue-Langevin (ILL), Grenoble, France, ftp://ftp.ill.fr/pub/cs/.

[40]Y.S. Touloukian (Ed.), Thermophysical Properties of Matter [The TPRC Data Series—A Comprehensive Compilation of Data]: Vol. 12, Thermal Expansion: Metallic Elements and Alloys; Vol. 13, Thermal Expansion–Nonmetallic Solids. IFI/Plenum, New York, 1970–79.

[41]E. Zimmermann, R. Weiss, M. Witthaut, and D. Neushutz, "Interdiffusion Paths in the Diffusion Couple Ti–SiC," *Mater. Res. Adv. Tech.*, **89**, 10 (1998).

[42]J. J. Moore and H. J. Feng, "Combustion Synthesis of Advanced Materials: Part I, Reaction Parameters," *Prog. Mater. Sci.*, **39**, 243–72 (1995).

[43]H. Baker (Ed.), *ASM Handbook*, Vol. 3, *Alloy Phase Diagrams*. ASM International, Materials Park, OH, 1992.

[44]M. W. Barsoum, T. El-Raghy, L. Farber, M. Amer, R. Christini, and A. Adams, "The Topotactic Transformation of Ti_3SiC_2 into a Partially Ordered Cubic $Ti(C_{0.67}Si_{0.06})$ Phase by the Diffusion of Si into Molten Cryolite," *J. Electrochem. Soc.*, **146** [10] 3919–23 (1999).

[45]C. Racault, F. Langlais, and R. Naslain, "Solid-State Synthesis and Characterization of the Ternary Phase Ti_3SiC_2," *J. Mater. Sci.*, **29**, 13 (1994).

[46]E. H. Kisi and D. P. Riley, "*In Situ* Diffraction Thermometry and Differential Thermal Analysis," *J. Appl. Crystallogr.*, in press.

[47]Y. Du and J. C. Schuster, "Experimental Investigation and Thermodynamic Calculation of the Titanium–Silicon–Carbon System," *J. Am. Ceram. Soc.*, **83** [1] 197–203 (2000).

[48]S. Arunajatesan and A. H. Carim, "Synthesis of Titanium Silicon Carbide," *J. Am. Ceram. Soc.*, **78** [3] 667–72 (1995). □